Surfatron and Stochastic Acceleration of Electrons at Supernova Remnant Shocks

K. G. McClements,[1] M. E. Dieckmann,[2] A. Ynnerman,[2] S. C. Chapman,[3] and R. O. Dendy[1]
[1]*EURATOM/UKAEA Fusion Association, Culham Science Centre, Abingdon, Oxfordshire, OX14 3DB, United Kingdom*
[2]*Institute of Technology and Natural Science, Linköping University, Campus Norrköping, 601 74 Norrköping, Sweden*
[3]*Department of Physics, University of Warwick, Coventry CV4 7AL, United Kingdom*
(Received 27 March 2001; published 30 November 2001)

The surfatron offers the possibility of particle acceleration to arbitrarily high energies, given a sufficiently large system. Surfatron acceleration of electrons by waves excited by ions reflected from supernova remnant (SNR) shocks is investigated using particle simulations. It is shown that surfatron and stochastic acceleration could provide a seed population for the acceleration of cosmic ray electrons at SNR shocks.

DOI: 10.1103/PhysRevLett.87.255002 PACS numbers: 52.65.Rr, 52.35.Fp, 52.35.Qz, 98.70.Sa

Synchrotron emission from supernova remnants (SNRs) indicates the presence of highly relativistic electrons in such objects [1]. The diffusive shock mechanism [2] provides an efficient means of accelerating electrons at SNR shocks from a mildly relativistic threshold, but the problem of raising electrons to this threshold is unsolved. A possible solution is provided by the surfatron, proposed in [3] as a laser-plasma accelerator which can in principle produce electrons of arbitrarily high energy (unlike, for example, the beat-wave scheme [4]). It has been difficult to exploit fully the potential of the surfatron in laboratory experiments, which are necessarily restricted in size. However, the large spatial scales of SNRs suggests that the surfatron should be examined as a possible source of energetic particles in such plasmas. Ions reflected from SNR shocks can excite large amplitude electrostatic waves [5,6], an essential ingredient of the surfatron. The physics of charged particle interactions with large amplitude waves has a strong bearing on the confinement of α particles in controlled fusion devices [7], as well as having astrophysical applications.

Consider an electrostatic wave $E = E_x = E_0 \sin(kx - \omega t)$ ($E_y = E_z = 0$) propagating perpendicular to a magnetic field B in the z direction. An electron with $v_x \simeq v_\phi \equiv \omega/k$ can be trapped by the wave. In the zero phase velocity frame there is an electric field

$$E_y' = \gamma_\phi (E_y - v_\phi B/c) = -\gamma_\phi v_\phi B/c\,, \qquad (1)$$

where $\gamma_\phi = (1 - v_\phi^2/c^2)^{-1/2}$ and c is the speed of light. An electron is accelerated continuously by this field if it remains trapped, which requires $E_0 > \gamma_\phi B$ [3]. Previous authors have considered electrons remaining close to the bottom of the wave potential, in which case [3]

$$v_y = v_\phi \Omega_e t (1 + \Omega_e^2 t^2 v_\phi^2/c^2)^{-1/2}/\gamma_\phi\,, \qquad (2)$$

where Ω_e is the electron gyrofrequency. For $v_\phi \ll c$, Eq. (2) indicates that an electron is accelerated to $v \sim c$ in a time $\tau_{\rm acc} \sim c/(v_\phi \Omega_e)$. This analysis is based on the assumption of a plane wave unaffected by the electrons. Particle-in-cell (PIC) [6] and Vlasov [8] simulations indicate that the lifetime of a monochromatic wave is limited by sideband instabilities. For the surfatron to be effective B must be low enough for electrons to be trapped (so that $E_0 > \gamma_\phi B$), but high enough that they undergo significant acceleration in the lifetime of the wave [Eq. (2)]. Moreover, Eq. (2) is only strictly applicable to deeply trapped electrons. PIC simulations [6] indicate that trapped electrons generally lie close to the separatrix of the trapped-particle island: one cannot then treat v_x as constant and Eq. (2) is not strictly valid.

Here we present a self-consistent study of the surfatron using a PIC code and parameters which are representative of SNR shocks. The simulations have one space dimension and three velocity dimensions. We use periodic boundary conditions, so that the only modes represented have wave numbers $k = 2\pi n/L$ where L is the box size and n is an integer. The simulation box has 90 cells (each of length 204 cm) in a simulation with $L = \lambda_0$, the wavelength of a Buneman instability [5], and 360 cells in a simulation with $L = 4\lambda_0$. In the former there are more than 10^5 electrons per cell: to determine acceleration efficiency, it is desirable to have the best possible statistical representation of the electron population. Simulations such as those with $L = \lambda_0$, which exclude wave vectors other than those of a linearly unstable mode and multiples thereof, provide a link between theory and real plasmas and make it possible to study individual nonlinear processes.

The electrons are initially Maxwellian with temperature 10^5 K and density $n_e \simeq 120$ cm^{-3}: these values are consistent with observations of "lobe" regions close to the young SNR SN1987A [9], for example. The simulation magnetic field is 3.5×10^{-4} G. Achterberg and Ball [10] have inferred minimum B values upstream of the shock associated with SN1978K in the range 2.5×10^{-6} to 2.5×10^{-4} G. The ion (proton) population consists initially of a Maxwellian component, with temperature 10^7 K, and two beams, propagating in opposite directions at speeds $v_b = 0.06c$ perpendicular to B. The wavelength of the Buneman-unstable mode is then $\lambda_0 = 2\pi v_b/\omega_{\rm pe}$ where $\omega_{\rm pe}$ is the electron plasma frequency [5]. The beams are Maxwellian, with temperatures of 10^7 and 1.7×10^9 K. The existence of ion beams upstream of high Mach

number quasiperpendicular shocks is indicated by hybrid [11] and full particle [12] simulations. The number density of each beam is $n_e/6$, giving a concentration comparable to reflected ion fractions observed in hybrid simulations [11]. Such simulations indicate that the reflected ion speed in the upstream plasma frame is of the order of the shock speed v_s. Thus, our simulations are applicable to shocks with $v_s \sim 0.06c$: observations show that efficient electron acceleration occurs at shocks with v_s exceeding $\sim(0.01 - 0.03)c$ and that supernova shock speeds can exceed $0.03c$ [1].

We first present results from the simulation with $L = \lambda_0$. The ion beam propagating in the positive x direction excites a Buneman instability at $\omega \simeq \omega_{\rm pe}$, $\tilde{k} \equiv k\lambda_0/2\pi = 1$. Figure 1 shows the evolution of the $\tilde{k} = 1$ electric field component E_0. After a phase of exponential growth, the wave fluctuates around 10^{-3} statvolt cm^{-1}, then collapses to about 3×10^{-4} statvolt cm^{-1} at $\omega_{\rm pe}t/2\pi \simeq 95$. Thereafter it remains at a similar amplitude before collapsing again at $\omega_{\rm pe}t/2\pi \simeq 160$. Surfatron acceleration is apparent when the electron v_y distribution is plotted versus time: this is shown in Fig. 2, with time normalized to $2\pi/\Omega_e(\omega_{\rm pe}/\Omega_e = 10^2)$. There is a linear feature of diminishing intensity extending from $v_y = 0$ to $v_y \simeq 0.4c$, which forms a bump-on-tail. Plots of the electron (x, v_x) phase space show results similar to those in [6]: as the wave grows, a trapped-particle island can be seen forming. Most of the trapped electrons remain close to the island separatrix, with only a few migrating towards the center. This accounts for the rapid fall in phase space density of the linear feature in Fig. 2 as the simulation progresses: the proximity of trapped electrons to the separatrix means that they are detrapped by small reductions in E_0. It is consequently essential to use a large number of particles in the simulation to determine the highest energies to which electrons are accelerated.

Figure 3 depicts the evolution of waves in the simulation with $L = 4\lambda_0$, $\omega_{\rm pe}/\Omega_e = 10^2$. As the amplitude of the Buneman wave at $\tilde{k} = 1$ builds up, harmonics of this appear. After $\omega_{\rm pe}t/2\pi \simeq 40$, the initial wave and its harmonics are replaced with a continuum: this can be attributed to sideband instabilities, initially at $\tilde{k} = 0.75$, 1.25, and subsequently at other $\tilde{k}$. Setting $E_0 \propto \tilde{k}^{-\alpha}$, we obtain $\alpha \simeq 2.3$ at high $\tilde{k}$. At $0.25 \lesssim \tilde{k} \lesssim 1$, where the spectrum departs from a power law, there are several modes of comparable amplitude. These have $\omega \sim \omega_{\rm pe}$, and therefore the phase speed of the longest wavelength mode ($\tilde{k} = 0.25$) is $v_\phi \sim 4 \times \omega_{\rm pe}\lambda_0/2\pi \simeq 0.24c$. The electron (x, v_x) phase space at $\omega_{\rm pe}t/2\pi \simeq 43$, shortly after the appearance of the continuous $\tilde{k}$ spectrum, is shown in Fig. 4. In contrast to the single trapped-particle island observed when $L = \lambda_0$, there is an interaction between several such islands. The v_x distribution in Fig. 4 extends up to the phase speed of the fastest-propagating mode, with $\tilde{k} = 0.25$. Figure 4 indicates acceleration of electrons in v_x due to interactions with several waves.

It is instructive to solve directly the equations of motion using parameters corresponding to Figs. 1 and 3. Solutions for the case of $L = \lambda_0$ are shown in Fig. 5. The wave amplitude, assumed constant, is taken to be 10^{-3} statvolt cm^{-1} (cf. Fig. 1). The solid curve indicates $v_y(t)$ for a trapped electron initially lying close to the island separatrix; the short dashed curve is the solution for an electron initially at the center of the island; the long dashed curve is the solution for an untrapped electron, initially just outside the separatrix. The two trapped electrons are accelerated uniformly at almost identical rates. As $v_y \to 0$ the slope of these curves is $dv_y/dt \simeq 0.06c\Omega_e$, consistent with Eq. (2) and with the slope of the linear feature in Fig. 2. The untrapped trajectory in Fig. 5 is a perturbed Larmor orbit.

Figure 6(a) shows a solution for parameters corresponding to those of the simulation with $L = 4\lambda_0$. The total

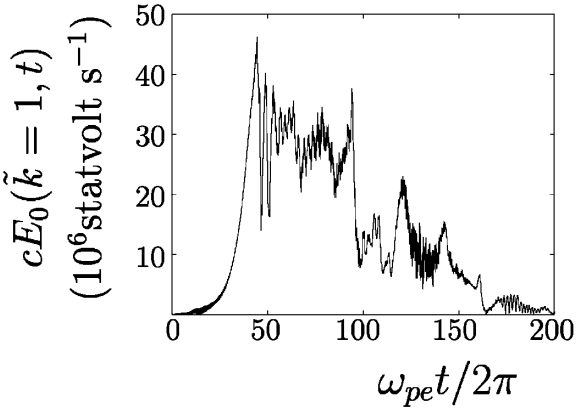

FIG. 1. Amplitude of waves with wavelength $\lambda = \lambda_0 \equiv 2\pi v_b/\omega_{\rm pe}$ in simulation with box size $L = \lambda_0$.

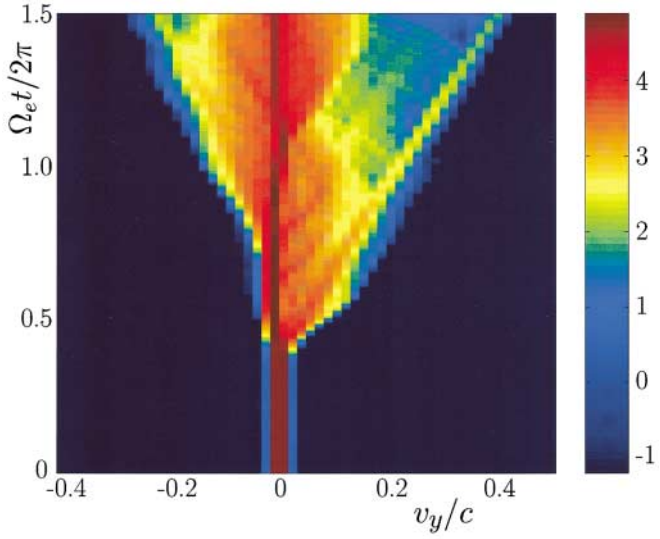

FIG. 2 (color). Time evolution of electron v_y distribution in simulation with $L = \lambda_0$. Colors from dark blue through dark red indicate increasing phase space density.

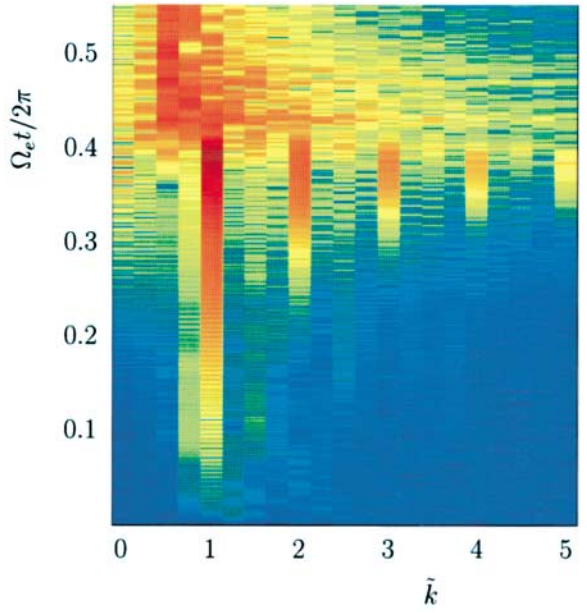

FIG. 3 (color). Evolution of wave spectrum in simulation with $L = 4\lambda_0$. Colors from dark blue through dark red indicate increasing wave amplitude.

integration time is $4\pi/\Omega_e$, and eight modes are included, with amplitudes and wave numbers approximately equal to those of the modes in Fig. 3 with $\tilde{k} \leq 2$ at $\Omega_e t/2\pi \simeq 0.4$: the amplitudes are assumed to be constant. The electron initially lies at the center of the trapped-particle island corresponding to the first wave excited, and remains trapped for long enough to be accelerated in v_y to about $0.1c$. Thus, surfatron acceleration can occur to a limited extent in the simulation. Because of the presence of several modes, the electron has a chaotic trajectory, and is thus more susceptible to detrapping than it would be if only one mode were present. After being detrapped, it executes a Larmor gyration before interacting again with the waves.

In the case of Fig. 6(b) ω/Ω_e has been increased by a factor of 10 (corresponding to $\omega_{\rm pe}/\Omega_e = 10^3$): the integration time and initial conditions are the same as in Fig. 6(a). The electron is first accelerated to $v_y \simeq 0.15c$ via the surfatron before it is detrapped. After a partial gyration, it is trapped again and undergoes a second phase of surfatron acceleration, up to $v \simeq 0.32c$, before being detrapped a second time. On a time scale greater than $\omega_{\rm pe}^{-1}$ there is acceleration in v_y at approximately constant v_x, as in Fig. 5: electrons are trapped for long enough to accelerate to energies higher than those found at lower $\omega_{\rm pe}/\Omega_e$. Although trajectories are still chaotic, electrons are less susceptible to detrapping because E_0/B is a factor of 10 higher. The assumption of constant mode amplitudes in this case would require the waves to exist for 2×10^3 plasma periods. The lifetime of the continuous spectrum in the simulation with $L = 4\lambda_0$ is unknown, since it was still present at the end of the simulation, and the parameters differ from those of Fig. 6(b). However, a similar spectrum observed in a simulation described in [8] persisted for at least 120 plasma periods without being driven: in our case the waves are driven and thus would be expected to last longer than those considered in [8].

Similar results are obtained for waves propagating at angles $\theta \neq 90°$ with respect to B. For a single mode, the surfatron is insensitive to θ if $|90° - \theta| \leq 15°$. When several modes are present, trajectories similar to those in Fig. 6 are obtained for a wide range of values of θ. The key result that a stochastic form of the surfatron appears when $\omega_{\rm pe}/\Omega_e > 10^2$ is thus valid in the case of $\theta \neq 90°$. The form of the trajectories is insensitive to the number of modes, provided that there are at least several of them.

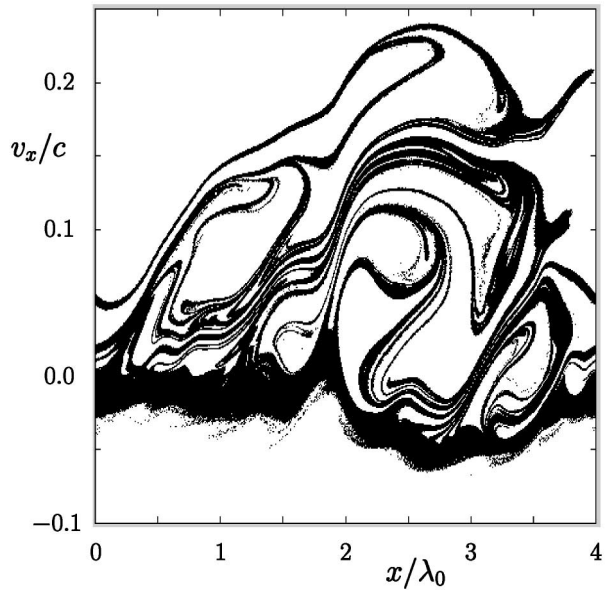

FIG. 4. Electron distribution in (x, v_x) space at $\omega_{\rm pe}t/2\pi = 43$ in simulation with $L = 4\lambda_0$.

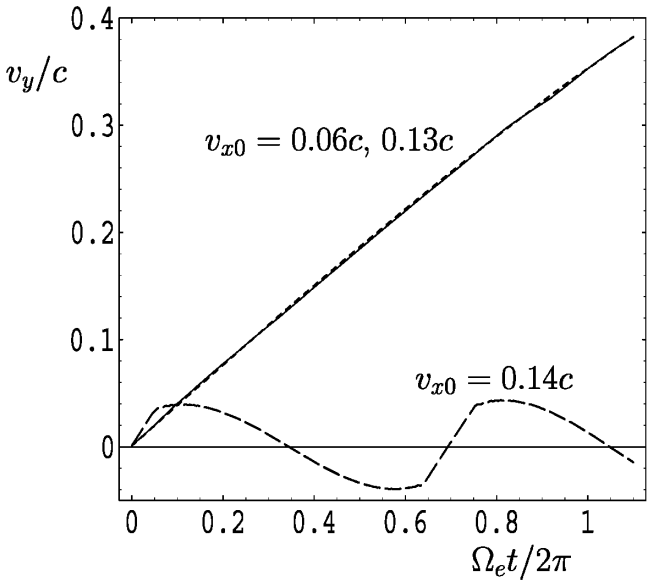

FIG. 5. Orbits for parameters of simulation with $L = \lambda_0$.

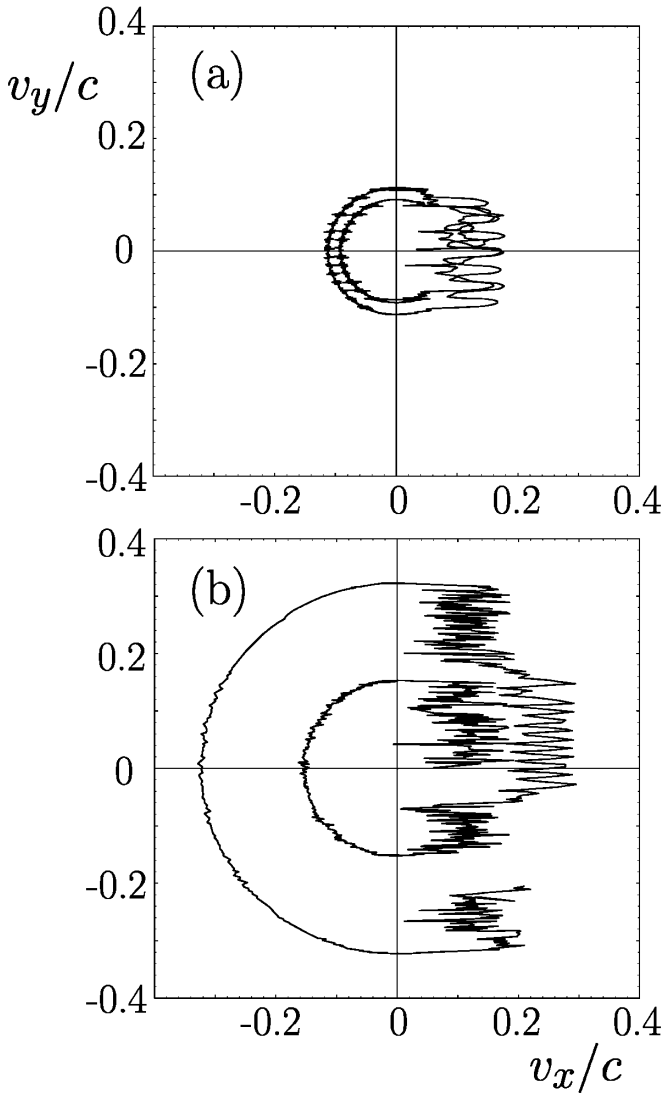

FIG. 6. (a) Orbits for parameters of simulation with $L = 4\lambda_0$. (b) As in (a) except that $\omega_{\rm pe}/\Omega_e = 10^3$.

In conclusion, we have used a PIC code to carry out self-consistent studies of electron acceleration under conditions prevailing at SNRs. Large amplitude electrostatic waves are driven via the Buneman instability by ion beams, known to be associated with high Mach number quasiperpendicular shocks. In a simulation with $\omega_{\rm pe} = 100\Omega_e$, in which wave numbers k other than that of the initial instability and multiples thereof were suppressed, some electrons trapped by the waves were accelerated up to about $c/2$ via the surfatron. The trapped electron fraction is sensitive to the wave amplitude, which collapses after a few tens of plasma periods. In a more realistic simulation, in which k was not restricted to multiples of the linearly unstable wave number, a sequence of sideband instabilities occurred, giving rise to a continuum in k. Electrons were accelerated along the wave propagation direction, up to the phase velocity of the wave with the minimum k. Surfatron acceleration is ineffective in this case, due to electron detrapping. However, a stochastic version of the surfatron reappears when $\omega_{\rm pe}/\Omega_e > 10^2$: if the waves remain for at least a few cyclotron periods, electrons can then be trapped for long enough to be accelerated to mildly relativistic energies. The true range of values of $\omega_{\rm pe}/\Omega_e$ at SNR shocks is difficult to determine, but estimates of n_e and B in [9,10] suggest that $\omega_{\rm pe}/\Omega_e \gg 1$.

Earlier simulations [5] indicate that strong stochastic acceleration can occur when $\omega_{\rm pe}/\Omega_e$ is as low as 10, but in this case the surfatron is unimportant. It would be desirable to carry out simulations with $\omega_{\rm pe}/\Omega_e \gg 10^2$, to determine whether stochastic surfatron acceleration can occur in this régime. This is computationally difficult since the surfatron time scales with $1/\Omega_e$ while the time step in the code is determined by $1/\omega_{\rm pe}$. It would also be desirable to simulate two space dimensions, so that an angular distribution of waves could be represented, or to increase the simulation box size and hence the resolution in k space: one would then expect to observe high ω modes with lower k and higher v_ϕ. Figure 4 suggests that this would result in higher electron energies, even without surfatron acceleration. Our results indicate that a combination of surfatron and stochastic acceleration is likely to play a key role in producing mildly relativistic electrons at SNR shocks, particularly when $\omega_{\rm pe} \gg \Omega_e$.

The National Supercomputer Centre (NSC) of Sweden provided the computer resources used to carry out this work. It was supported by the Commission of the European Communities (under TMR Network Contract No. ERB-CHRXCT980168), the University of Linköping, the U.K. Department of Trade and Industry, and EURATOM.

[1] P. L. Biermann and J. P. Cassinelli, Astron. Astrophys. **277**, 691 (1993).
[2] A. R. Bell, Mon. Not. R. Astron. Soc. **182**, 147 (1978).
[3] T. Katsouleas and J. M. Dawson, IEEE Trans. Nucl. Sci. **30**, 3241 (1983).
[4] T. Tajima and J. M. Dawson, Phys. Rev. Lett. **43**, 267 (1979).
[5] M. E. Dieckmann *et al.,* Astron. Astrophys. **356**, 377 (2000).
[6] M. E. Dieckmann *et al.,* Phys. Plasmas **7**, 5171 (2000).
[7] H. L. Berk *et al.,* Phys. Plasmas **3**, 1827 (1996).
[8] M. Brunetti *et al.,* Phys. Rev. E **62**, 4109 (2000).
[9] J. M. Blondin and P. Lundqvist, Astrophys. J. **405**, 337 (1993).
[10] A. Achterberg and L. Ball, Astron. Astrophys. **285**, 687 (1994).
[11] K. B. Quest, J. Geophys. Res. **91**, 8805 (1986).
[12] N. Shimada and M. Hoshino, Astrophys. J. Lett. **543**, L67 (2000).